To cite this version:

Vitola Pasetto, Leticia and Richard, Romain and Pic, Jean-Stéphane and Manero, Marie-Hélène and Violleau, Frédéric and Simon, Valérie *Ozone Quantification by Selected Ion Flow Tube Mass Spectrometry: Influence of Humidity and Manufacturing Gas of Ozone Generator.* (2019) Analytical Chemistry, 91 (24). 15518-15524. ISSN 0003-2700

Ozone Quantification by Selected Ion Flow Tube Mass Spectrometry: Influence of Humidity and Manufacturing Gas of Ozone Generator

Leticia Vitola Pasetto,[†,‡] Romain Richard,[†] Jean-Stéphane Pic,[§] Marie-Hélène Manero,[†] Frédéric Violleau,[‡] and Valérie Simon*[,‡]

[†]Laboratoire de Génie Chimique, Université de Toulouse, CNRS, INPT, UPS, 31432 Toulouse, France
[‡]Laboratoire de Chimie Agro industrielle, LCA, Université de Toulouse, INRA, 31030 Toulouse, France
[§]TBI, Université de Toulouse, CNRS, INRA, INSA, 31077 Toulouse, France

ABSTRACT: The quantification of ozone by SIFT MS was investigated in conditions suitable with an industrial emission context (high ozone demand, dry air/oxygen as the manufacturing gas of the ozone generator, and high humidity levels beyond saturation at room conditions). Ozone reacts with four negative precursor ions available in the SIFT MS device (NO_2^-, O_2^-, HO^-, and O^-), each precursor ion having its specific domain of linearity. For a high ozone concentration range, only NO_2^- and O_2^- have resulted in a linear behavior (between 1 and 100 ppmv of O_3 for NO_2^-, between 1 and 50 ppmv of O_3 for O_2^-). No water interference was identified during ozone measurements by SIFT MS using NO_2^- and O_2^- precursor ions, even with extreme humidity levels. The presence of nitrogen oxide contaminants (due to the use of dry air as the manufacturing gas of the ozone generator) affected the ozone quantification by SIFT MS. It is critical for NO_2^- precursor ions, whose rate constant varied as a function of NO_2 concentrations. With O_2^- precursor ion, ozone was successfully measured in the presence of nitrogen oxides; however, the secondary chemistry must be taken into account.
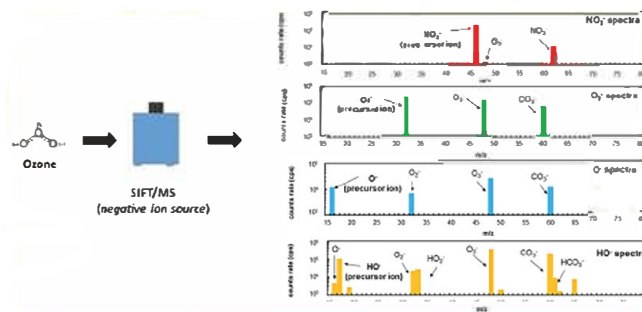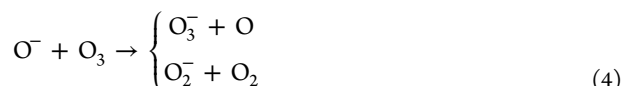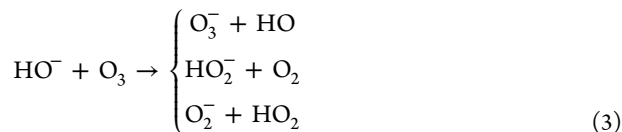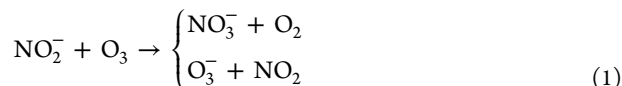
Besides its crucial role in controlling the UV radiation in the upper atmosphere, ozone (O_3) is an important primary oxidant employed in chemical treatment processes. Because of its high oxidation potential, ozone has been applied worldwide in water treatment for disinfection and removal of color, taste, odor, and micropollutants in drinking water.[1] It is also employed in advanced oxidation processes (AOP) to treat emerging pollutants in wastewater treatments.[2,3] Furthermore, some studies have revealed that ozonation can remove volatile organic compounds (VOCs) from gaseous effluents[4] and is able to reduce the odor intensity by removing specific components.[5]

In this chemical treatment context, ozone is usually generated in the gas phase by plasma/corona discharge (when an air or oxygen flow passes through two electrodes under high voltage) or by UV lamps (at wavelengths under 200 nm).[6–8] As higher ozone concentrations are produced by plasma discharge, this technique is frequently applied in studies with industrial conditions.[2,5,9,10] However, when air is fed into the ozone generator (corona discharge), the presence of contaminants such as nitrogen oxides has been identified.[11,12]

Ozone is commonly analyzed using UV analysis (at 254 nm wavelength), by iodometric or by indigo colorimetric studies.[6,9,13] In parallel to these traditional analytical methods, only a few studies have investigated the measurement of ozone

concentrations by mass spectrometry based techniques, such as selected ion flow tube (SIFT MS)[11] and ion trap.[14]

Particularly in an industrial context, SIFT MS has emerged as an interesting technique because it is able to analyze in real time a wide variety of compounds at trace levels in gas phase through an ionization reaction with H_3O^+, NO^+, and O_2^+.[15–18] In recent years, five negative ions (NO_2^-, NO_3^-, O_2^-, HO^-, and O^-) have been integrated to the range of precursor ions available for analysis of samples, broadening the list of compounds analyzed by SIFT MS[19]—adding among them ozone, which can only react with negative precursor ions because its proton affinity is smaller than water (625.5 vs 691 kJ mol^{-1}).[20] The quantification of neutral compounds by SIFT MS is based on soft ionization reaction with precursor ions, carried out in a region with fixed conditions (temperature, pressure, and reaction time).[15,21] According to Williams et al.,[11] ozone reacts with four negative precursor ions available in the SIFT MS device (NO_2^-, O_2^-, HO^-, and O^-), being only unreactive to NO_3^-. The ionization of O_3 usually proceeds via charge and O atom transfer, as shown in eq 1 for NO_2^-, eq 2 for O_2^-, eq 3 for HO^-, and eq 4 for O^-.

$$NO_2^- + O_3 \rightarrow \begin{cases} NO_3^- + O_2 \\ O_3^- + NO_2 \end{cases} \tag{1}$$

$$O_2^- + O_3 \rightarrow O_3^- + O_2 \tag{2}$$

$$HO^- + O_3 \rightarrow \begin{cases} O_3^- + HO \\ HO_2^- + O_2 \\ O_2^- + HO_2 \end{cases} \tag{3}$$

$$O^- + O_3 \rightarrow \begin{cases} O_3^- + O \\ O_2^- + O_2 \end{cases} \tag{4}$$

Previous studies in the 1970s and 1980s investigated the reaction between ozone and negative ions applying different experimental techniques (such as flowing afterglow[22,23] and ion beam methods[24]). Dotan et al.[23] studied the reaction between O_3 and OH^- and reported the conversion of O_3^- ion to CO_3^- and O_2 in the presence of CO_2 (with a rate constant of 5.5×10^{-10} cm^3 molecule^{-1} s^{-1}). In addition to the rate constant of O_2^- ion and ozone, Fahey et al.[22] reported the cluster formation in the presence of humidity, in which $O_2^- \cdot (H_2O)_{n\ 1,2,3,4}$ ions would react with O_3 by a considerable fast charge transfer and the water molecule transfer (10^{-10} cm^3 molecule^{-1} s^{-1}). Cluster formations in SIFT MS happen via sequential three body association, in which the molecule of the carrier gas acts as a stabilizing agent.[25] The nature of the carrier gas in the reaction chamber (flow tube) may influence the cluster formation and therefore modify its related rate coefficients.

The objective of this work was to explore in more detail the quantification of ozone by SIFT MS in the context of industrial gas emission. Industrial gaseous effluents are usually a mixture of several compounds, often presenting high humidity levels, in which ozone based treatment systems apply quite high ozone concentrations (several hundred ppmv). The determination of the rate coefficient was one of the objectives of this study because the SIFT MS device was employed under different operating conditions than those reported in the literature:[11] a higher temperature of the flow tube and a different carrier gas (nitrogen). Moreover, the present study investigated the impact of the humidity and the effect of the nature of the manufacturing gas (oxygen or dry air for ozone generator) on ozone quantification by SIFT MS.

MATERIALS AND METHODS

Ozone and Humid Air Generation. Ozone was generated by a plasma discharge ozone generator (HTU500 AZCO Industries Limited, Canada) fed by oxygen (99.999%, Linde Gas, France) and by dry air (dew point equal to −40 °C at 101.3 kPa), which was produced by an air compressor (ZR55, oil free air ISO 8573 1 class 0, Atlas Copco France) integrated to an air filter (Olympian Plus, Norgren, U.K.). Ozone concentration could vary from 370 ppmv to 4000 ppmv with dry air and from 760 ppmv to 4800 ppmv with oxygen, depending on the gas flow and the generator power. Ozone concentrations were measured directly after its production by an UV analyzer (BMT 964, BMT MESSTECHNIK GMBH, Germany). The calibration was performed between 1 ppmv and 100 ppmv (at 6 levels) from the dilution of ozone air or ozone oxygen stream into an air stream, whose gas flows were

controlled by mass flowmeters (SLA 5850S B Brooks Instruments, U.S.A.).

A humidification system (Serv'Instrumentation, France) was employed to generate calibrated humidity levels from 0.01%vol of H_2O (dry air, dew point equal to −40 °C at 101.3 kPa) until 4.00%vol of H_2O (dew point equal to 29 °C at 101.3 kPa), at five different levels of humidity. Since the range from 2.00 to 4.00%vol of H_2O was higher than the saturation at room conditions (20 °C and 101.3 kPa), the system was heated at 40 °C by a heated circulating oil bath (Model 1160S, VWR, U.S.A.), composed of a stainless steel smooth coil immersed in a synthetic thermoliquid (Ultra 350, Lauda, Germany) installed at the air line after the humidification system. The gas line between the mixture point and the SIFT MS was isolated and heated using a heated cable (FGR 100, Omegalux, France) to prevent condensation. The estimated residence time of gas in the system (between the mixture point and SIFT MS device) was 2 s.

SIFT-MS Analysis. The SIFT MS device applied in this study (Voice 200*ultra*, Syft Technologies Ltd., New Zealand) produced the negative precursor ions by microwave discharge using wet conditions for HO^- and O_2^- and using dry conditions for NO_2^- and O^-. Only one precursor ion was selected at a time by a first quadrupole mass filter and was then injected to the reaction chamber (flow tube) by a nitrogen flow (180 NmL min^{-1}) as carrier gas, whereas the sample was introduced by a calibrated capillary at 20 NmL min^{-1}. In the flow tube (kept at 119 °C and 0.07 kPa), the analyte (neutral compound) reacted with a selected precursor ion and generated product ions with specific mass to charge ratios (m/z) that were quantified by a second quadrupole mass spectrometer, calculating a count rate per second (signal intensity in cps).[11,15]

The analyte concentration in the flow tube ($[A]_{ft}$ in molecules cm^{-3}) was calculated by eq 5, which depends on the rate coefficient (k in cm^3 molecule^{-1} s^{-1}) of the reaction between the neutral compound and the precursor ion, on the ratio between the precursor ion count rate at time equal to 0 ($[I_0]$ in cps) and at time t ($[I]$ in cps) and the reaction time in the flow tube (t in s) (considered equal to 5 ms for the Syft model used in this study). In case of a monoconstituent and $m/z < 100$, the product ion count rate ($[P]$) can be expressed as the difference between $[I_0]$ and $[I]$. eq 5 in function of $[P]$ leads to eq 6.

$$\ln\left(\frac{[I_0]}{[I]}\right) = k[A]_{ft}t \tag{5}$$

$$\frac{[P]}{[I]} = \frac{1 - e^{-k[A]_{ft}t}}{e^{-k[A]_{ft}t}} \tag{6}$$

A critical point on applying SIFT MS analysis is the condition of linear correlation between $[P]$ and $[A]_{ft}$. It is only valid for low concentrations of analytes, and hence, the precursor ion is only slightly consumed.[15] This linear correlation between $[P]/[I]$ and $[A]_{ft}$ was obtained rearranging the eq 6 to eq 8, when the limit of $k[A]_{ft}t$ approaching zero was considered in the exponential expression (eq 7), neglecting the differential diffusion between precursor and product ions.

$$\lim_{k[A]_{ft}t \to 0} \frac{(1 - e^{-k[A]_{ft}t})}{e^{-k[A]_{ft}t}} = k[A]_{ft}t \tag{7}$$

$$\frac{[P]}{[I]} = k[A]_{ft}t \tag{8}$$

In Figure 1, it is clear that the linear correlation between $[P]$ and $[A]_{ft}$ is only valid for $[P]/[I] < 1$. Knowing the $[A]_{ft}$ and
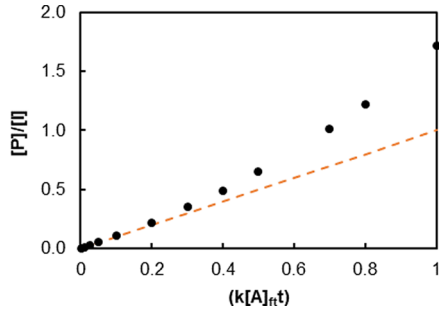
Figure 1. Comparison between the linear eq 8 (dotted line) and the exponential correlation represented by eq 6 (●).

the operating conditions of the flow tube, the analyte concentration in the sample ($[A]_{sample}$ in ppmv) could be calculated by eq 9, where T_{ft} (K) is the flow tube temperature, P_{ft} (kPa) is the flow tube pressure, φ_s is the sample flow (NmL min^{-1}), φ_c is the carrier gas flow (NmL min^{-1}), and k_b the Boltzmann constant (equivalent to the ratio of the ideal gas constant by the Avogadro number, i.e., 1.4×10^{-20} kPa cm^3 molecule^{-1} K^{-1}).

$$[A]_{sample} = [A]_{ft} \frac{T_{ft}k_b 10^6}{P_{ft}} \frac{(\varphi_s + \varphi_c)}{\varphi_s} \tag{9}$$

In the same way that analyte concentration was calculated by eq 5, the rate coefficient could also be obtained. It represents

the slope of the linear correlation of $\ln(([P]+[I])/[I])$ vs $[A]_{ft}t$, if the $[A]_{sample}$ and, consequently, $[A]_{ft}$ are known. In the case when more than one product ion is generated, the branching ratio of each product ion can also be obtained from eq 5. When all product ion count rates were summed in $[P]$, a global rate coefficient was obtained. Whereas, when only the count rate of one of the product ions was considered to calculate $[P]$, a partial rate coefficient was acquired. The ratio between the partial and the global rate coefficient represents the branching ratio of the specific product ion.

The limit of detection (LOD) in SIFT MS analysis was calculated considering the confidence level equal to three standard deviations above background (eq 10), as the limit of quantification (LOQ) is the lowest concentration that can be measured with a precision of ±20%[26,27] (eq 11). b_μ represents the mean background count rate of the product ion at a specific m/z ratio (cps); t_m the time of measurement (s); and s the sensitivity (cps ppbv^{-1}), which represents how many product ions (cps) at the specific m/z ratio were produced for a given concentration of analyte. In this study, b_μ and t_m were calculated from a blank analysis, i.e., without the presence of the analyte (O_3).

$$LOD_{ppbv} = \frac{3\sqrt{b_\mu t_m}}{st_m} \tag{10}$$

$$LOQ_{ppbv} = \frac{25 + 5\sqrt{25 + 4b_\mu t_m}}{2st_m} \tag{11}$$

■ RESULTS AND DISCUSSION

Linearity Range of Negative Ion Precursors as a Function of Ozone Concentration. The respective spectra
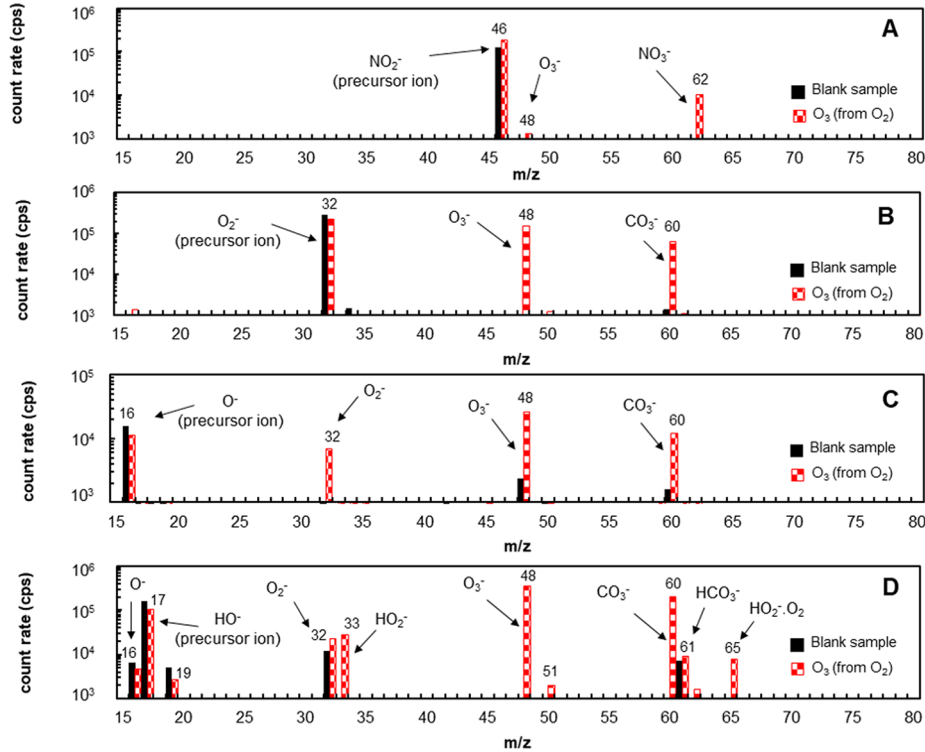
Figure 2. Comparison between a blank analysis (black solid bars) and sample containing 75 ppmv of O_3 generated by oxygen (red dashed bars). (A) NO_2^- precursor ion spectra. (B) O_2^- precursor ion spectra. (C) O^- precursor ion spectra and (D) HO^- precursor ion spectra.

Table 1. Rate Coefficients, LOD, and LOQ for Ozone Generated by Oxygen and Dry Air

		ozone			
		by oxygen			by dry air
precursor	product ions [branching ratio]	k^a	LOD^b	LOQ^b	k^a
NO_2^-	$NO_3^- + O_2$ [0.92]	0.12 ± 0.02	45	80	0.22 ± 0.04
	$O_3^- + O_2$ [0.08]				
O_2^-	$O_3^- + O_2$	1.3 ± 0.2	4	6	1.3 ± 0.1
	$O_3^- + CO_2 \rightarrow CO_3^- + O_2$				
	$O_3^- + NO_2 \rightarrow NO_3^- + O_2$				

$^a 10^{-9}$ cm^3 molecule^{-1} s^{-1}. ^{b}ppbv.

for each of the four negative precursor ions reactive to ozone[11] are represented in Figure 2. They were obtained during full scan (FS) mode and individually for each precursor ion. In FS mode, the second quadrupole spectrometer scans over a mass range covering from 15 to 250 m/z, calculating a count rate for each unit of m/z. In Figure 2, the comparison of two different samples is shown: the blank sample (black bars) is obtained only when dry air is fed into SIFT MS flow tube, and the second trace (red bars) is when 75 ppmv of O_3 is produced from oxygen and diluted in air.

In agreement with Williams et al.,[11] the reaction between NO_2^- precursor ion and O_3 generated mostly the NO_3^- [m/z 62] product ion, with a slight generation of O_3^- [m/z 48], through a charge transfer mechanism (Figure 2A).

In the case of O_2^-, O^-, and HO^- precursor ions, besides the expected product ions O_3^- [m/z 48], O_2^- [m/z 32] (for O^- and HO^- precursor ions), and HO_2^- [m/z 33] (for HO^- precursor ion); CO_3^- [m/z 60] ion was also detected (Figure 2B,C,D). The CO_3^- generation is a result of the natural occurrence of CO_2 in air (around 400 ppmv)[28] as shown by Dotan et al.[23] while studying secondary chemistry of O_3-. Since a part of O_3^- [m/z 48] product ions reacts with CO_2 in the flow tube, the product ion CO_3^- [m/z 60] must also be considered as a secondary reaction of O_3^- [m/z 48] and be counted for the quantification of ozone by O_2^-, O^-, and HO^- precursor ions.

However, the intensity signal of O^- (Figure 2C) and HO^- (Figure 2D) precursor ions were less important than the sum of product ions (O_3^- [m/z 48]; O_2^- [m/z 32]; HO_2^- [m/z 33]; CO_3^- [m/z 60] and HCO_3^- [m/z 61]), resulting in $[P]/[I] \gg 1$ (equal to 3.9 for O^- and 5.9 for HO^-, considering the sum of all product ions). Consequently, O^- and HO^- precursor ions were out of the linearity domain when the ozone concentration in the sample was at 75 ppmv (75% of the maximum level of the studied range) for the flow tube conditions applied in this study (i.e., for a mixing ratio of the sample into the flow tube equal to 10%). Only NO_2^- and O_2^- precursor ions have shown the potential to be linear in the ozone concentration range studied ($[P]/[I]$ was equal to 0.06 for NO_2^- and to 0.97 to O_2^- at 75 ppmv of O_3). However, it was expected that the O_2^- precursor ion would not present a linear relation during all the ozone concentration range, because from 0.75, $[P]/[I]$ shows a considerable deviation from the linear expression (Figure 1).

Rate Coefficients of NO_2^- and O_2^- with Ozone. The rate coefficients of O_2^- and NO_2^- precursor ions with O_3 (shown in Table 1) were obtained using nitrogen as carrier gas, a flow tube temperature at 392 K and considering the ozone generated by oxygen and later diluted in air (at 5 levels of humidity). They were calculated by eq 5, where O_3^- [m/z 48]

and CO_3^- [m/z 60] product ions were considered for O_2^- precursor ion and O_3^- [m/z 48] and NO_3^- [m/z 62] product ions were counted for NO_2^- precursor ion. The rate coefficient of O_2^- obtained in this study ($1.3 \pm 0.2 \times 10^{-9}$ cm^3 molecule^{-1} s^{-1}) is in good agreement with Williams et al.[11] (equal to 1.3×10^{-9} cm^3 molecule^{-1} s^{-1}), whereas in the case of NO_2^- rate coefficient, the value reported by Williams et al.[11] (0.18×10^{-9} cm^3 molecule^{-1} s^{-1}) is slightly higher than the one found in this study ($0.12 \pm 0.02 \times 10^{-9}$ cm^3 molecule^{-1} s^{-1}). We have also reported a slightly higher contribution of the charge transfer mechanism (equal to 8%) than the 1% presented by Williams et al.[11] The uncertainty of the rate coefficients was calculated by the method of error propagation, considering the error from the linearity regression and from the ozone/humid air generation (estimated as <10%).

The ozone concentrations measured by SIFT MS when applying the rate coefficients of NO_2^- and O_2^- of Table 1 are shown in Figure 3. Concentrations calculated from NO_2^-
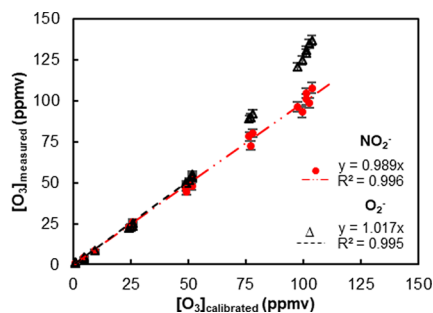

Figure 3. Comparison between the calibrated ozone concentrations with those measured by NO_2^- precursor ion (red ●) and O_2^- precursor ion (Δ).

precursor ion are in excellent agreement with the calibrated ozone concentrations (slope = 0.989 in Figure 3), whereas from O_2^- precursor ion, it shows a deviation for concentrations higher than 50 ppmv of O_3. The falsely high concentrations could be explained by elevated values of $[P]/[I]$, which suggests that O_2^- precursor ion was out of the linear range for ozone concentrations values higher than 50 ppmv (the slope until 50 ppmv was equal to 1.017 in Figure 3).

The LOD of SIFT MS (Table 1) for measuring ozone (generated by oxygen) by O_2^- precursor ions is lower than by NO_2^- (with a measurement time equal to 60 s), which reflects the difference of sensitivity of SIFT MS between the two precursor ions. For NO_2^- precursor ion, SIFT MS detected 170 cps ppmv^{-1} of O_3; whereas for O_2^- precursor ion, it measured 2770 cps ppmv^{-1} of O_3.

Effect of Humidity. The influence of the humidity in the measurement of ozone concentrations by SIFT MS was investigated in a large range of H_2O concentrations (0.01 to 4.00%vol) and for all five levels of ozone concentration between 1 and 100 ppmv. All repetitions of the 5 levels of humidity for each condition of ozone concentration are plotted in Figure 3, and no considerable dispersion is observed. It suggests that the quantification of ozone by NO_2^- and O_2^- precursor ions were not affected by humidity, which was confirmed by the analysis of $[P]/[I]$ ratios for both precursor ions at a fixed ozone concentration (75 ppmv) as a function of H_2O concentration (Figure 4). The $[P]/[I]$ ratios did not significantly vary with the increase of humidity, in agreement with the analysis previously evidenced from Figure 3.
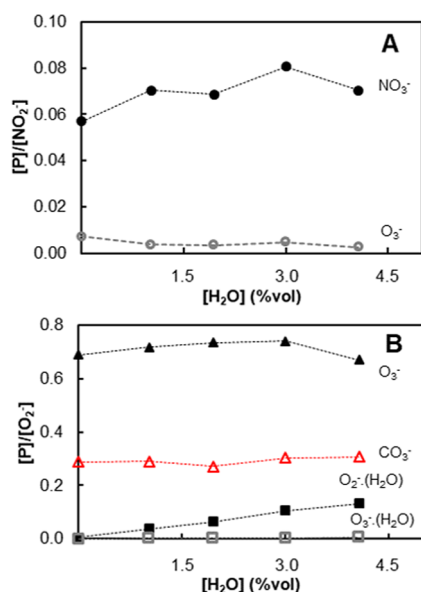
Figure 4. $[P]/[I]$ of the product ions as a function of humidity at 75 ppmv of O_3. (A) NO_2^- precursor ion with NO_3^- [m/z 62] (●) and O_3^- [m/z 48] (○). (B) O_2^- precursor ion with O_3^- [m/z 48] (▲); CO_3^-[m/z 60] (red △); $O_2^-\cdot(H_2O)$ [m/z 50] (■) and $O_3^-\cdot(H_2O)$ [m/z 66] (□).

According to Figure 4B, the formation of the cluster $O_2\cdot$ (H_2O) [m/z 50] from the precursor ion O_2^- increased with humidity. However, the ratio between the cluster $O_3^-\cdot(H_2O)$

[m/z 66] (generated from product ion O_3^-) and O_2^- count rate was negligible even with the highest H_2O concentration. The contrast behavior of water clusters compared to those proposed by Fahey et al.[22] could be explained by a different experimental technique applied and by the use of helium as carrier gas in the previous studies. Assuming that the water cluster generation for negative ions follows a three body mechanism similar to positive ions, the use of nitrogen may have reduced the rate coefficient of the three body reactions, minimizing the water cluster generation.

Effect of the Manufacturing Gas on Ozone Generator. In order to investigate the influence of NO_x contaminants on the ozone analysis by SIFT MS, a second ozone calibration was carried out. Ozone was generated by dry air and then diluted in air streams that contained five different levels of humidity. Some differences between the calibration when ozone was generated by oxygen and by dry air were identified. They are shown in Figure 5, where NO_2^- and O_2^- spectra of both samples containing the same concentration of ozone (75 ppmv) are compared. A higher intensity of NO_3^- [m/z 62] product ion was generated from NO_2^- precursor ion (Figure 5A) when ozone was produced by dry air. Regarding the O_2^- spectra (Figure 5B), a third product ion was detected, identified as NO_3^- [m/z 62].

The presence of NO_3^- on the O_2^- spectra leads to two main conclusions. First of all, it demonstrates the generation of NO_x contaminants when dry air is used as feed gas into the ozone generator[12] (NO_2 could be detected[29] thanks to the positive ion source integrated in SIFT MS device). Second, it indicates a secondary chemistry related to the O_3^- product ion as previously proposed by Ferguson,[30] in which O_3^- would react with NO_2, generating NO_3^- and O_2.

The rate coefficient between O_3 and O_2^- obtained from the ozone generated by dry air was similar to the rate obtained with oxygen, as shown in Table 1. For the dry air condition, the NO_3^- product ion must be considered as a secondary reaction of O_3^- since one part of O_3^- produced from O_3/O_2^- reaction reacts with NO_2 as well as with CO_2. As the rate coefficient has not varied, the domain of linearity for O_2^- precursor remains equivalent to the one found for ozone generated by oxygen, and thus, accurate quantification is only valid until 50 ppmv of O_3.

The rate coefficient calculated for the O_3/NO_2^- reaction was higher (around the double) when ozone was generated by dry
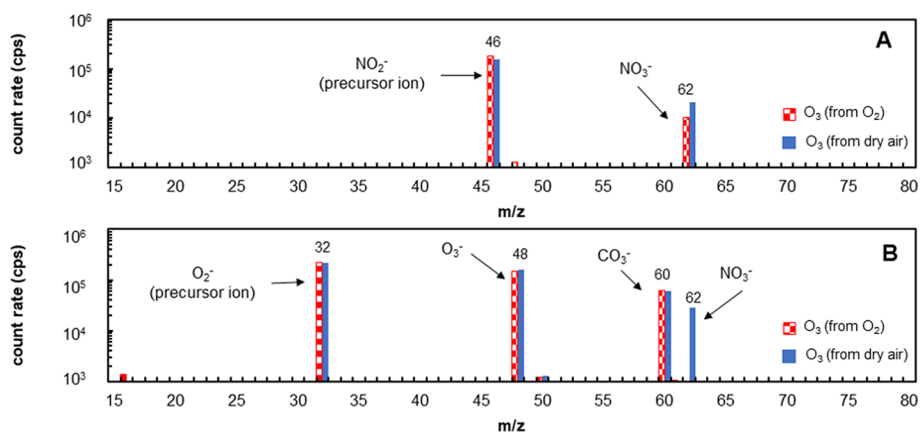
Figure 5. Comparison between both samples containing 75 ppmv of O_3 generated by oxygen (red dashed bars) and 75 ppmv of O_3 generated by dry air (blue solid bars). (A) NO_2^- precursor ion spectra. (B) O_2^- precursor ion spectra.

air compared to pure oxygen, as shown in Table 1. It suggests that NO_x contaminants interfere on NO_3^- [m/z 62] product ion, misrepresenting the rate coefficient of O_3/NO_2^- reaction. Furthermore, the apparent rate coefficient of O_3/NO_2^- (calculated individually for each condition of the calibration) has increased as a function of the concentration of nitrogen dioxide (NO_2), as shown in Figure 6. The NO_2 concentrations were obtained from the NO_2^+ [m/z 46] from O_2^+ precursor ion, applying the rate coefficient available in LabSyft kinetics database (release 1.6.2).[29]

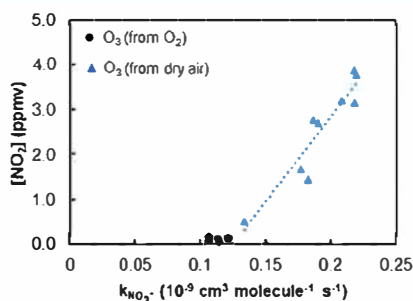Figure 6. Apparent rate coefficient of NO_2^- with O_3 generated by dry air (blue ▲) and by oxygen (●) as a function of the NO_2 concentration.

Since the rate coefficient of NO_2^- has shown a dependence with the concentration of NO_x contaminants, it seems to be more appropriate to measure ozone concentration from the O_2^- precursor ion (if both secondary reactions are considered). However, it is limited by the domain of linearity.

■ CONCLUSIONS

Ozone can be successfully measured by SIFT MS up to 100 ppmv, regardless of the humidity level of the sample. Four precursor ions can be used to measure ozone: NO_2^-, O_2^-, O^-, and HO^- with each precursor ion having its specific domain of linearity. For high ozone concentration ranges—the interest of this study—only NO_2^- and O_2^- have resulted in a linear behavior (between 1 and 100 ppmv of O_3 for NO_2^- and 1 and 50 ppmv of O_3 for O_2^- for the flow tube conditions applied in this study). In addition, no interference due to H_2O content was identified during ozone measurements by SIFT MS for both precursor ions, which is an interesting property because water interference has been reported in the literature during ozone measurements by an UV analyzer.[31]

Furthermore, the presence of nitrogen oxide contaminants and CO_2 affected the ozone quantification by SIFT MS. Therefore, secondary chemistry concerning the reaction of CO_2 and nitrogen oxides with O_3^- (characteristic product ion of O_3 with O_2^-) must be taken into account in order to accurately measure ozone concentration with O_2^- precursor ion. In the case of NO_2^- precursor ion, an overlapping with the ozone characteristic product ion was identified, incapacitating the use of NO_2^- precursor for ozone quantification in the presence of nitrogen oxides (ozone generator fed by dry air).

■ AUTHOR INFORMATION

Corresponding Author
* valerie.simon@ensiacet.fr. Tel. +33 5 34 32 35 52

ORCID ⓘ
Valérie Simon: 0000 0002 2624 157X

Author Contributions

The manuscript was written through contributions of all authors. All authors have given approval to the final version of the manuscript.

Notes

The authors declare no competing financial interest.

■ ACKNOWLEDGMENTS

■ REFERENCES

(1) Loeb, B. L.; Thompson, C. M.; Drago, J.; Takahara, H.; Baig, S. Ozone: Sci. Eng. 2012, 34 (1), 64−77.

(2) Ibáñez, M.; Gracia Lor, E.; Bijlsma, L.; Morales, E.; Pastor, L.; Hernández, F. J. Hazard. Mater. 2013, 260, 389−398.

(3) González Labrada, K.; Richard, R.; Andriantsiferana, C.; Valdés, H.; Jáuregui Haza, U. J.; Manero, M. H. Environ. Sci. Pollut. Res. 2018, DOI: 10.1007/s11356 018 3559 9.

(4) Monneyron, P.; Manero, M. H.; Manero, S. Can. J. Chem. Eng. 2007, 85 (3), 326−332.

(5) Bildsoe, P.; Adamsen, A. P. S.; Feilberg, A. Biosyst. Eng. 2012, 113 (1), 86−93.

(6) Christensen, P. A.; Yonar, T.; Zakaria, K. Ozone: Sci. Eng. 2013, 35 (3), 149−167.

(7) Summerfelt, S. T.; Hochheimer, J. N. Prog. Fish Cult. 1997, 59, 94−105.

(8) Li, X.; Zhang, G.; Pan, H. J. Hazard. Mater. 2012, 199−200, 255−261.

(9) Vega, E.; Martin, M. J.; Gonzalez Olmos, R. Chemosphere 2014, 109, 113−119.

(10) Skalska, K.; Ledakowicz, S.; Louwe, R.; Szymczak, R. Chem. Eng. J. 2017, 318 (2), 181−188.

(11) Williams, S.; Campos, M. F.; Midey, A. J.; Arnold, S. T.; Morris, R. A.; Viggiano, A. A. J. Phys. Chem. A 2002, 106, 997−1003.

(12) Pekárek, S. Acta Polytech. 2003, 43 (6), 47−51.

(13) Abou Saoud, W.; Assadi, A. A.; Guiza, M.; Bouzaza, A.; Aboussaoud, W.; Soutrel, I.; Ouederni, A.; Wolbert, D.; Rtimi, S. Chem. Eng. J. 2018, 344 (March), 165−172.

(14) Marshall, D. L.; Pham, H. T.; Bhujel, M.; Chin, J. S. R.; Yew, J. Y.; Mori, K.; Mitchell, T. W.; Blanksby, S. J. Anal. Chem. 2016, 88 (5), 2685−2692.

(15) Smith, D.; Španěl, P. Mass Spectrom. Rev. 2005, 24, 661−700.

(16) Huffel, K.; Van; Heynderickx, P. M.; Dewulf, J.; Van Langenhove, H. Chem. Eng. Trans. 2012, 30, 67−72.

(17) Vitola Pasetto, L.; Richard, R.; Pic, J. S.; Manero, M. H.; Violleau, F.; Simon, V. Int. J. Environ. Anal. Chem. 2019, DOI: 10.1080/03067319.2019.1650919.

(18) Vitola Pasetto, L.; Simon, V.; Richard, R.; Pic, J. S.; Violleau, F.; Manero, M. H. Chemosphere 2019, 235, 1107−1115.

(19) Hera, D.; Langford, V.; McEwan, M.; McKellar, T.; Milligan, D. Environments 2017, 4 (1), 16.

(20) Hunter, E. P. L.; Lias, S. G. J. Phys. Chem. Ref. Data 1998, 27 (3), 413−656.

(21) Guimbaud, C.; Catoire, V.; Bergeat, A.; Michel, E.; Schoon, N.; Amelynck, C.; Labonnette, D.; Poulet, G. Int. J. Mass Spectrom. 2007, 263, 276−288.

(22) Fahey, D. W.; Böhringer, H.; Fehsenfeld, F. C.; Ferguson, E. E. J. Chem. Phys. 1982, 76 (4), 1799−1805.

(23) Dotan, I.; Davidson, J. A.; Streit, G. E.; Albritton, D. L.; Fehsenfeld, F. C. J. Chem. Phys. 1977, 67 (6), 2874−2879.

(24) Rutherford, J. A.; Turner, B. R.; Vroom, D. A. J. Chem. Phys. 1973, 58 (12), 5267−5271.

(25) Španěl, P.; Smith, D. Rapid Commun. Mass Spectrom. 2000, 14, 1898−1906.

(26) Milligan, D. B.; Francis, G. J.; Prince, B. J.; McEwan, M. J. *Anal. Chem.* **2007**, *79* (6), 2537−2540.

(27) Francis, G. J.; Milligan, D. B.; McEwan, M. J. *Anal. Chem.* **2009**, *81* (21), 8892−8899.

(28) IPCC. *Climate Change 2013: The Physical Science Basis.* Contribution of Working Group I to the Fifth Assessment Report of the Intergovernmental Panel on Climate Change: Cambridge, United Kingdom and New York, NY, 2013.

(29) Španěl, P.; Smith, D. *Rapid Commun. Mass Spectrom.* **2000**, *14* (8), 646−651.

(30) Ferguson, E. E. *Can. J. Chem.* **1969**, *47*, 1815−1820.

(31) Wilson, K. L.; Birks, J. W. *Environ. Sci. Technol.* **2006**, *40* (20), 6361−6367.